The prediction and understanding of jet noise

By D. J. Bodony

1. Motivation and objectives

Despite identification of jet noise as an important byproduct of the newly invented jet engine (Morley 1939), and as an impediment to the incipient commercial jet aircraft industry in the 1950s (Lighthill 1952; Westley & Lilley 1952; Lassiter & Hubbard 1952; Lighthill 1954; Lassiter & Hubbard 1956), a completely satisfactory description of jet noise—that is, of the noise produced by the turbulent exhaust gases of a jet engine—has proven elusive. Two primary reasons for this difficulty are the lack of a universally agreed-upon theory of noise generation in turbulent flows and the challenge in taking experimental measurements in (often heated) high-speed jets.

Regardless, significant progress has been made on some of the theoretical descriptions of jet noise (Lighthill 1952, 1954; Lilley 1974; Goldstein 2003, to name but a few) and in its experimental characterization (Davies *et al.* 1963; Bradshaw *et al.* 1964; Tanna 1977*a*,*b*; Viswanathan 2004, for example). However, only recently have there been successful attempts at the numerical prediction of jet noise from first principles using large-eddy simulation (LES) and direct numerical simulation (DNS).

Much of the current jet noise work originates at the Center for Turbulence Research through its associated students or post-doctoral fellows (Boersma & Lele 1999; Constantinescu & Lele 2001; Freund 2001; Jansen *et al.* 2002; Bodony & Lele 2005*b*). The aforementioned studies have also been quite useful in establishing numerical databases for the continued exploration of noise source processes, both in general and as specifically applies to jets. This report documents some of the current efforts underway at CTR that are relevant to jet noise prediction and to its understanding, including both studies that are well documented and those that are in their early stages.

2. Cold and hot jets from subsonic to supersonic speeds

For the jet conditions listed in Table 1, large-eddy simulations were carried out in cylindrical coordinates for the filtered, compressible equations using non density-weighted variables. (See Bodony & Lele (2005*b*) for details.) The dynamic Smagorinsky model (Germano *et al.* 1991) was used to close the subgrid scale stresses. Sixth order optimized compact (Padé) finite difference schemes were used in the radial and axial directions; Fourier-spectral differencing was used in the azimuthal direction. Time integration used the low-dispersion, low-dissipation Runge-Kutta scheme of Stanescu & Habashi (1998). Forcing and absorbing sponges (Bodony 2005) provide boundary conditions on the computational boundaries. For all boundaries, the sponges absorb without reflection the outgoing vortical, entropic, and acoustic waves. At the inflow boundary, the sponge also induces jet unsteadiness by forcing disturbances formed by a normal-mode solution of the linearized stability equations for a spatially-growing disturbance on the inflow mean flow profile. Azimuthal mode number combinations, including $n = \pm 1, \ldots, \pm 4$, are random walked in time to provide broadband forcing without generation of unphysical noise;

the axisymmetric mode was not explicitly forced (Bodony & Lele 2002). The forcing amplitude, when summed over all modes, was $u_{\rm rms}/U_j = 0.03$.

The initial mean axial velocity profile, specified at $x/r_0 = 0$, was of the form

$$\frac{U}{U_j} = \frac{1}{2}\left(1 - \tanh\left[\frac{1}{4\theta_0}\left\{\frac{r}{r_0} - \frac{r_0}{r}\right\}\right]\right).$$

where θ_0, the initial momentum thickness, is a parameter. In all calculations $\theta_0/D_j = 0.045$. Assuming constant static pressure and known jet centerline temperature T_j the density was found from the Crocco-Busemann relation. The reference solution used in the sponge zones was found from Reynolds-averaged Navier-Stokes solutions of the parabolized Navier-Stokes equations using the v^2-f turbulence model (Choi & Lele 2001). A schematic of the computational domain, with sponge zones identified, is given in Fig. 1. Also shown in Fig. 1 are the bounding cylindrical surfaces of the Kirchhoff surface used to extrapolate the sound to the far-field, beyond the LES computational domain. Set at a distance of $R_s = 5D_j$, the Kirchhoff surface predictions are insensitive to the choice of R_s. The cylindrical surface is open with the upstream and downstream surfaces ignored. Although their absence may be accounted (Freund *et al.* 1996) the current results are instead restricted to polar angles in the range of $20° \leq \Theta \leq 150°$.

Figure 2 shows the centerline axial velocity U_c as a function of axial position using the Witze (1974) scaling to remove the jets' axial elongation with increasing M_j. (Note that $\kappa = 0.08(1 - 0.16M_j)(\rho_\infty/\rho_j)^{0.22}$.) In these coordinates the present calculations, along with those of Bogey *et al.* (2003) and Freund (2001), collapse onto a single curve which over-predicts the centerline velocity decay rate as measured by Tanna (1977*a*) and by others. The increased rate of change of U_c with x is believed to be caused by the relatively thick initial shear layers of the calculations, with $0.01 < \theta_0/D_j \leq 0.045$, compared with those found in experiment of $\theta_0 \sim 10^{-3}D_j$ (Viswanathan & Clark 2004). From the root-mean-square of centerline axial velocity (not shown) the LES data is found to over-predict the experimental data by $0.01U_j$ (3–4%). The discrepancy between the numerical and experimental data is believed to be related to the influence of the initially thick shear layers, which lack realistic turbulence.

The overall sound pressure level (OASPL) predictions of the calculations are shown in Fig. 3 for all of the jets in Table 1. In general, the LES data of higher-speed jets better predicts the experimentally measured sound pressure levels than do simulations of lower-speed jets. In the case of a low-speed heated jet (M05TR176), the jet noise predictions differ substantially from their measured values. The pressure spectra for each of these jets are found, in those cases in which the OASPL predictions agree with the experimental data, to be low-pass filtered versions of the experimental spectra. In most cases the maximum frequency available in the simulations was around $St = fD_j/U_j = 1.2$.

For the three highest-speed jets (M09TR086, M15TR056, and M15TR230), the agreement in the acoustic far-field to the experimental data justified additional investigation of the numerical databases. Of particular interest was the ability of Lighthill's acoustic analogy to predict the radiated noise of these high-speed jets. Then the analogy is used to explore reasons why a high-speed jet, with $U_j/a_\infty > 0.7$, becomes quieter when heated. Note that two of the jets (M15TR056 and M15TR230) have the same jet velocity and differ only by temperature.

ID	TID	U_j/a_∞	U_j/a_j	T_j/T_∞	M_c	$Re^\ddagger$	$N_r \times N_\theta \times N_x$
M05TR176	sp23	0.50	0.38	1.76	0.21	27,000	$128 \times 32 \times 240$
M05TR095	sp3	0.50	0.51	0.95	0.25	79,000	,,
M09TR270	sp46	0.90	0.55	2.70	0.34	13,000	,,
M09TR086	sp7†	0.83	0.90	0.86	0.43	88,000	,,
M15TR230	sp39	1.47	0.97	2.30	0.58	84,000	,,
M15TR056	sp62	1.47	1.95	0.56	0.83	336,000	$128 \times 32 \times 256$

TABLE 1. Conditions of the simulations presented. The nomenclature sp$N$, where N is an integer, listed in the 'TID' column, refers to conditions tabulated in Tanna (1977*a*). †The conditions for run M09TR086 are approximately the same as those used by Tanna (1977*a*). ‡The Reynolds numbers, with $Re = \rho_j U_j D_j/\mu_j$, are those used in the present LES and are not the same as in the experiments.

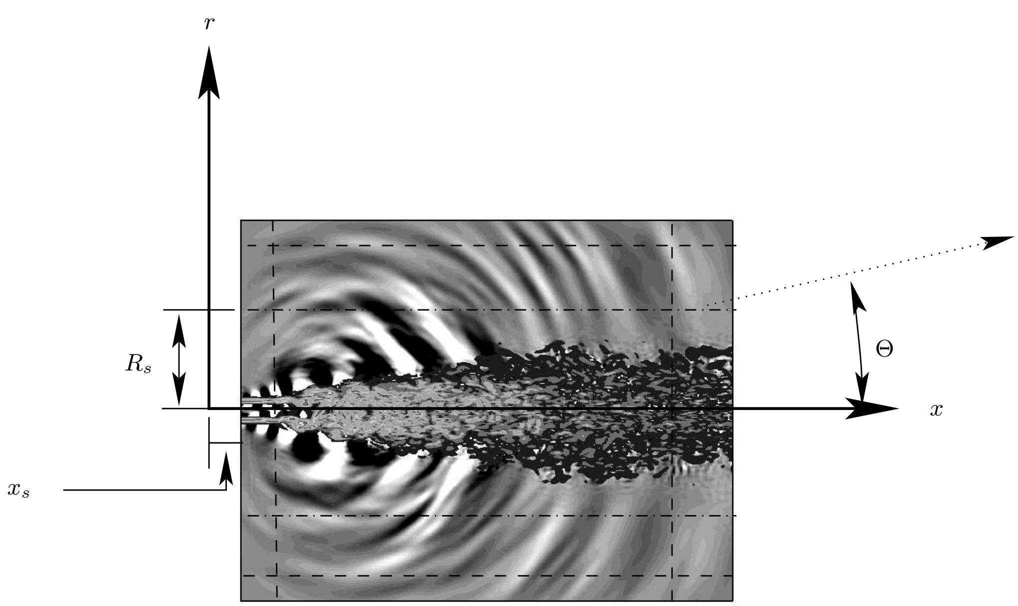

FIGURE 1. Schematic of calculation domain showing major features. The central region contains the LES domain and the sponge ($--$) and Kirchhoff surface surfaces ($-\cdot-$).

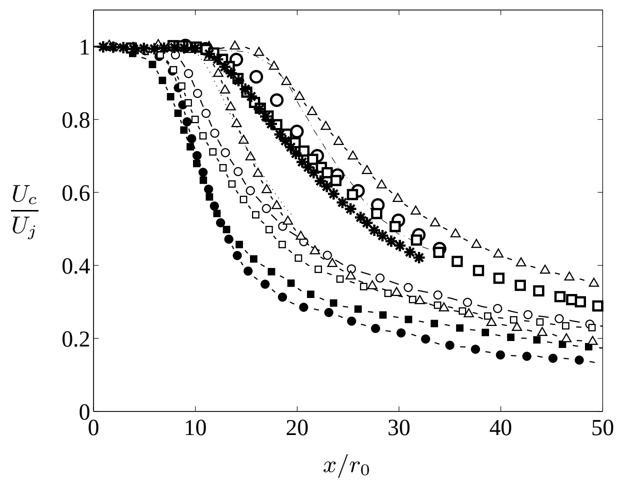

(a) Unscaled abscissa

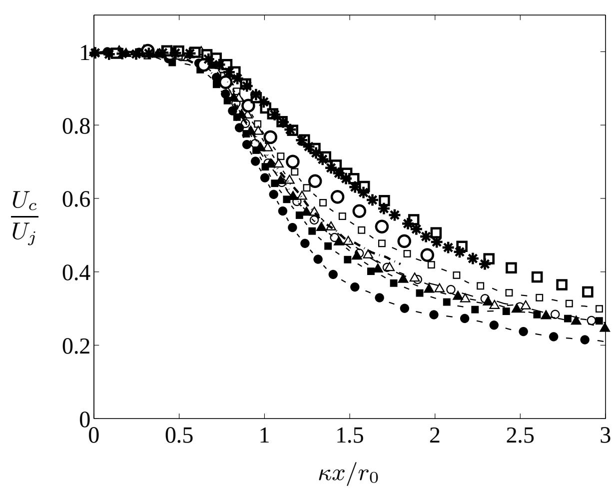

(b) Scaled abscissa

FIGURE 2. Centerline axial velocity in unshifted and in scaled and shifted Witze coordinates. Numerical data: $-\circ-$, M09TR086; $-\bullet-$, M09TR270; $-\square-$, M05TR095; $-\blacksquare-$, M05TR176; $-\triangle-$, M15TR056; $-\blacktriangle-$, M15TR230; $-\cdot-$, Freund (2001); $--$, Bogey *et al.* (2003). Experimental data: $\circ$, Tanna (M09TR086); $\square$, Bridges & Wernet (2003) (M05TR095); $\bigstar$, Crow & Champagne (1971) (incompressible).

As described in more detail in Bodony & Lele (2005*a*), the Lighthill predictions were remarkably close to the direct sound predictions from the large-eddy simulations. Figures 4 and 5 demonstrate the agreement for the two observer locations of $\theta = 30°$ and $90°$.

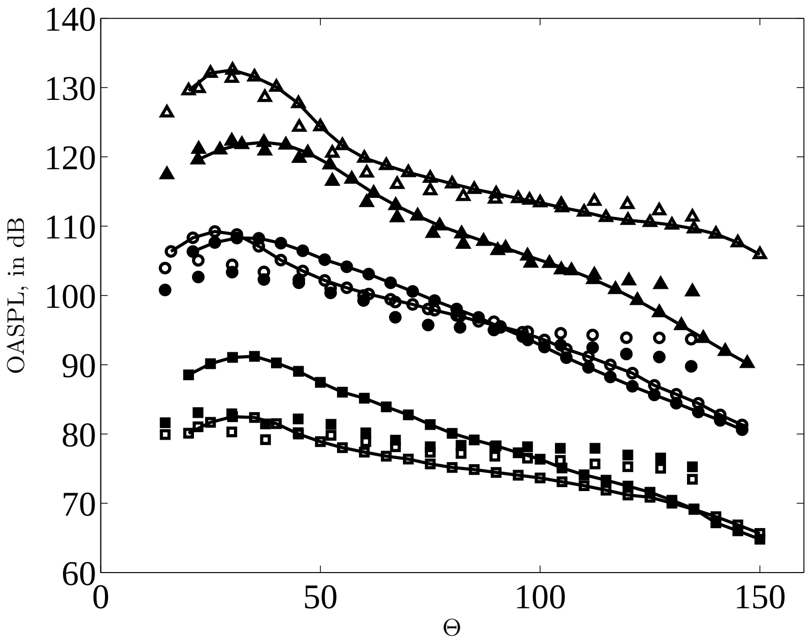

FIGURE 3. Overall sound pressure levels for all six simulated jets at a common distance of $100D_j$. Legend: −□−, M05TR095; −■−, M05TR176; − ∘ −, M09TR086, − • −, M09TR270; −△−, M15TR056; −▲−, M15TR230. Experimental data: □, Tanna (M05TR095); ■, Tanna (M05TR176); ∘, Tanna (M09TR086); •, Tanna (M09TR270); △, Tanna (M15TR056); ▲, Tanna (M15TR230).

3. Imperfectly expanded supersonic jets

A more recent extension of the pressure-matched jets discussed in the previous section concerns the presence of shock-cells within the early stages of the jet when operated at off-design conditions. When the jets are turbulent the interaction of the shock cells with the jet turbulence—both along the jet shear layers and downstream of the potential core collapse—is a significant source of noise. This shock-associated noise has been characterized experimentally (Harper-bourne & Fisher 1973; Tanna 1977*b*; Seiner & Norum 1979, 1980; Seiner & Yu 1981; Norum & Seiner 1982) and theoretically by Tam & Tanna (1982); Tam *et al.* (1985); Tam (1987, 1990), and more recently by Ray *et al.* (2004). A summary of shock-associated noise is given by Tam (1995). From the experimental studies it is known that the broadband shock associated noise is preferentially directed upstream towards the jet nozzle, resulting in a measurable increase in the overall sound pressure levels (OASPLs) for cold jets. For angles closer to the downstream jet axis the shock associated noise contributes less to the OASPL but is visible in the acoustic spectra.

In this study, the multiple-scales solution of Tam *et al.* (1985) is used to prescribe stationary shock cells into the large-eddy simulations (LES) of supersonic jets. The shock cell solution is used as an inlet boundary condition to jet calculations, and no special shock capturing numerical techniques are used.

For a cold jet with Mach number $M_j = 2.2$ and design Mach number of $M_d = 2.0$, the instantaneous dilatation and vorticity magnitude fields are shown in Fig. 6. The shock cells are visible in the initial portions of the jet, prior to the collapse of the potential core. The jet's pressure fluctuations are collected along a cylindrical surface parallel to the jet

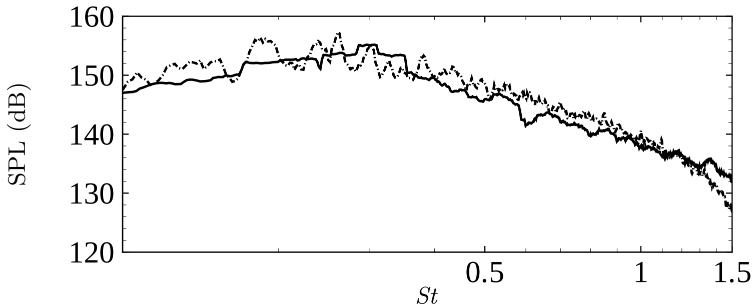

(a) $\Theta = 30^\circ$

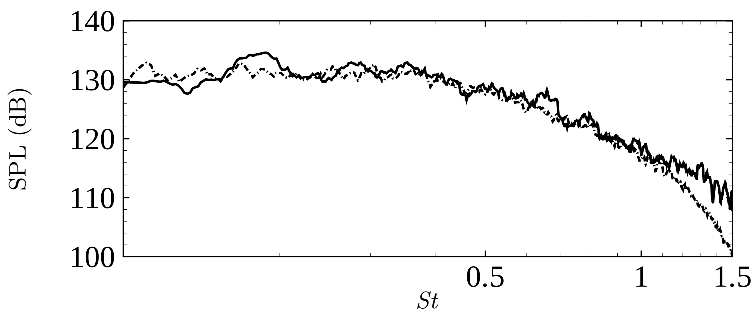

(b) $\Theta = 90^\circ$

FIGURE 4. Narrowband spectra at $\mathcal{R} = 30D_j$ for the Mach 2.0 unheated jet M15TR056. Lighthill (total), ——; Kirchhoff Surface, $- \cdot -$.

at a distance of $6D_j$ from the jet centerline. The OASPL for the pressure mismatched jet and the corresponding pressure matched jet (with $M_j = 1.95$ and described in detail in Bodony & Lele (2005*b*)) are shown in Fig. 7. Although taken close to the jet the data appear to show an increased upstream radiated noise level with some moderate increase in the downstream noise. Accompanying spectra, shown in Fig. 8, taken at three locations on this surface demonstrate that in the upstream direction, the imperfectly expanded jet shows increased sound near a frequency of $St = fD_j/U_j = 0.2$–0.3. At larger angles, in the downstream jet direction, the noise enhancement due to shock-associated noise occurs primarily for $St > 0.5$.

4. Human phonation

An effort was started in late 2005 to use the experience gained in jet noise prediction of industrial jets for the prediction of human speech (phonation). As described in Titze (2000), the primary source of voice production stems from the pulsing of the glottal jet (which has a diameter-based Reynolds number approaching 10,000) by the vibrating vocal folds, which oscillate with a fundamental frequency around 125–200 Hz for adults. Turbulence in the glottal jet, complex modal vibrations of the vocal folds, and reshaping of the cavity defined by the mouth and tongue contribute to the generation and

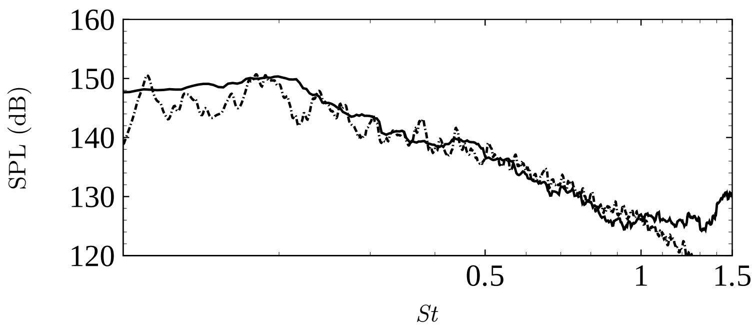

(a) $\Theta = 30°$

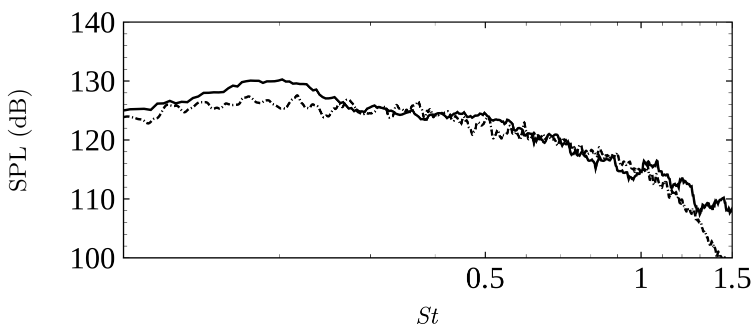

(b) $\Theta = 90°$

FIGURE 5. Narrowband spectra at $\mathcal{R} = 30D_j$ for the Mach 1.0 heated jet M15TR230. Lighthill (total), ——; Kirchhoff Surface, – · –.

selection of harmonics and broadband noise, the addition of which greatly enhances the 'pleasantness' of the voice.

Beyond this description very little is known about the fundamental processes of sound generation by the glottal jet. For example, the relative importance of the pulsating jet and the glottal jet turbulence is not well known, nor is there much evidence of the influence the mouth and tongue have on the sound generation. The relation between the vocal fold dynamics and the resulting sound harmonics is also ill-understood.

Some answers to these questions will arise from simulations of the vocal folds, with structural modeling, coupled to the trachea (including the larynx and glottal jet), mouth and tongue. Realistic geometric data will come from CT (Computed Tomography) scan measurements of human vocal tracts and will be modeled using the immersed boundary method (Ghias *et al.* 2004). Comparisons are planned for prediction of the sound \pa\, the first syllable in Parviz, with measurements taken on human participants.

5. Conclusions and future work

There are strong and active studies of jet noise being performed under the guidance and support of CTR. Industrial and medical applications are represented. In both classes, fundamental sound-generation questions remain to be answered.

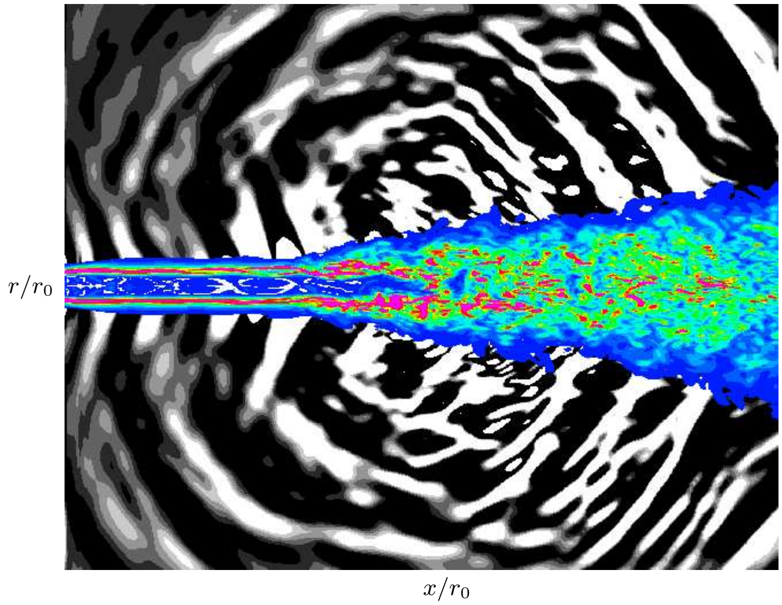

FIGURE 6. Instantaneous dilatation (background) and vorticity magnitude (near image) for a $M_j = 2.2$ ($M_d = 2.0$) cold jet. The shock cells are visible within the early regions of the jet. $r_0 = D_j/2$ is the jet radius.

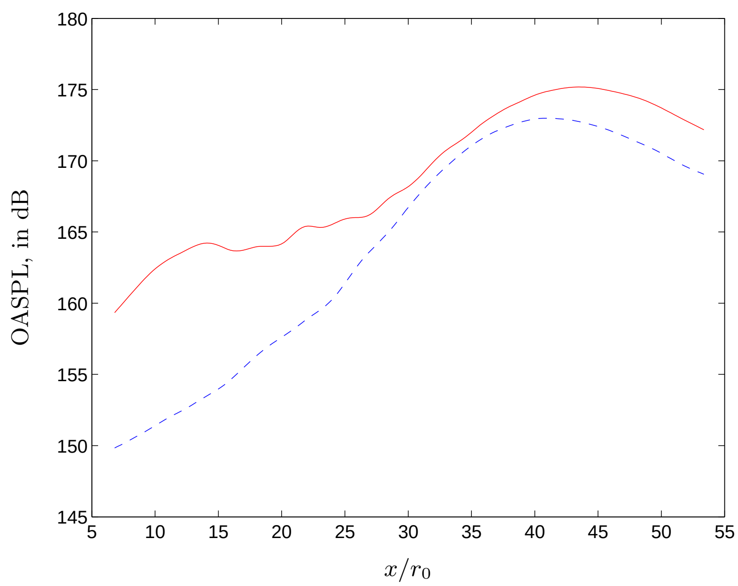

FIGURE 7. Overall sound pressure levels recorded along a cylindrical surface at a distance of $6D_j$ from the jet centerline. Pressure matched jet with $M_j = 1.95$, – –; imperfectly expanded jet —.

It has been found that lower speed jets, both heated and unheated, are sensitive to the conditions specified at the computation inlet. In particular, the correct disturbances introduced into the initial shear layers are not yet known. As the jet Mach number increases, the sensitivity to the inlet conditions decreases. Using relatively thick initial shear

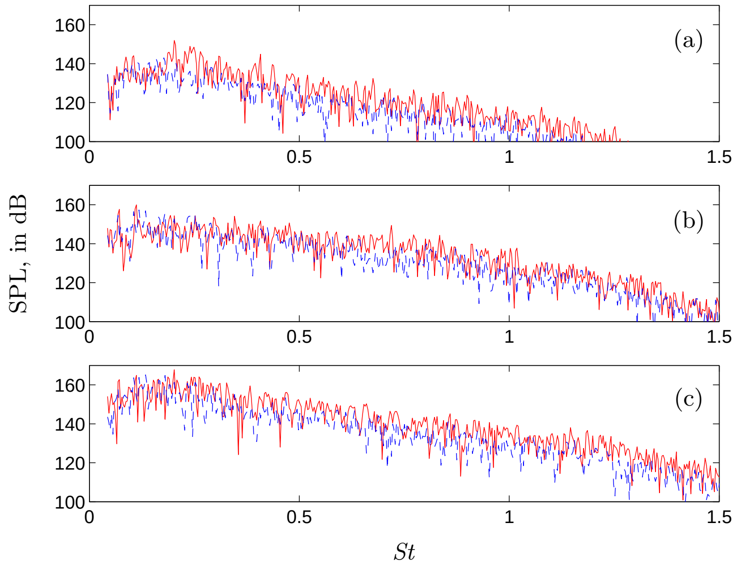

FIGURE 8. Sound pressure levels at $r/D_j = 6$ corresponding to Fig. 7. Pressure matched jet with $M_j = 1.95$, – –; imperfectly expanded jet ——. Spectrum measured at (a) $x/r_0 = 15.7$, (b) $x/r_0 = 30.0$, (c) $x/r_0 = 44.3$.

layers, reasonable turbulence and sound predictions were obtained. With the introduction of shock-cells into a jet simulation, the increased noise due to the shock-turbulence interactions appears to be qualitatively captured by the LES; a quantitative comparison is not yet available.

The relative success of the prediction of noise for industrial jets suggests that the human phonation study is within current capabilities. However, the low-speed jet sensitivity to inlet conditions demands that the glottal jet calculations proceed with strict attention to the environment immediately surrounding the vocal folds.

Acknowledgments

DJB gratefully acknowledges the following people. The pressure-matched jet noise work has been conducted with Professor S. K. Lele. The shock-cell noise study is on-going work with J. Ryu, P. K. Ray, and Professor Lele. The human phonation work is directed by Professor Rajat Mittal of George Washington University.

REFERENCES

BODONY, D. J. 2005 Analysis of sponge zones for computational fluid mechanics. *J. Comp. Phys.*, in press.

BODONY, D. J. & LELE, S. K. 2002 Large eddy simulation of turbulent jets and progress towards a subgrid scale turbulence model. In *Proceedings of International Workshop on LES for Acoustics*, DGLR-Report-2002-03, October 7–8, 2002, Göttingen, Germany.

BODONY, D. J. & LELE, S. K. 2005*a* Generation of low frequency sound in turbulent jets. *AIAA-2005-3041*.

Bodony, D. J. & Lele, S. K. 2005*b* On using large-eddy simulation for the prediction of noise from cold and heated turbulent jets. *Phys. Fluids* **17** (085103).

Boersma, B. J. & Lele, S. K. 1999 Large eddy simulation of a Mach 0.9 turbulent jet. *AIAA-1999-1874*.

Bogey, C., Bailly, C. & Juvé, D. 2003 Noise investigation of a high subsonic, moderate Reynolds number jet using a compressible LES. *Theor. Comp. Fluid. Dyn.* **16**, 273–297.

Bradshaw, P., Ferriss, D. H. & Johnson, R. F. 1964 Turbulence in the noise-producing region of a circular jet. *J. Fluid Mech.* **19**, 591–624.

Bridges, J. & Wernet, M. P. 2003 Measurements of the aeroacoustic sound source in hot jets. *AIAA-2003-3130*.

Choi, M.-R. & Lele, S. K. 2001 Prediction of shock-cell structure using parabolized stability equations. *AIAA-2001-0744*.

Constantinescu, G. S. & Lele, S. K. 2001 Large eddy simulation of a nearly sonic turbulent jet and its radiated noise. *AIAA-2001-0376*.

Crow, S. C. & Champagne, F. H. 1971 Orderly structure in jet turbulence. *J. Fluid Mech.* **48**, 547–591.

Davies, P. O. A. L., Fisher, M. J. & Barratt, M. J. 1963 The characteristics of the turbulence in the mixing region of a round jet. *J. Fluid Mech.* **15**, 337–367.

Freund, J. B. 2001 Noise sources in a low-Reynolds-number turbulent jet at Mach 0.9. *J. Fluid Mech.* **438**, 277–305.

Freund, J. B., Lele, S. K. & Moin, P. 1996 Calculation of the radiated sound field using an open Kirchhoff surface. *AIAA J.* **34**, 909–915.

Germano, M., Piomelli, U., Moin, P. & Cabot, W. H. 1991 A dynamic subgrid-scale eddy viscosity model. *Phys. Fluids A* **3**, 1760–1765.

Ghias, R., Mittal, R. & Lund, T. S. 2004 A non-body conformal grid method for simulation of compressible flows with complex immersed boundaries. *AIAA-2004-0080*.

Goldstein, M. E. 2003 A generalized acoustic analogy. *J. Fluid Mech.* **488**, 315–333.

Harper-bourne, M. & Fisher, M. J. 1973 The Noise from shock waves in supersonic jets. In *Proceedings No. 131 of the AGARD Conference on Noise Mechanisms*, Brussels, Belgium.

Jansen, K., Maeder, T. & Reba, R. 2002 Finite-element based large-eddy simulation of the near-nozzle region of a compressible round jet. *AIAA-2002-2358*.

Lassiter, L. W. & Hubbard, H. H. 1952 Experimental studies of noise from subsonic jets in still air. *NACA TN-2757*.

Lassiter, L. W. & Hubbard, H. H. 1956 The near noise field of static jets and some model studies of devices for noise reduction. *NACA Report 1261*.

Lighthill, M. J. 1952 On sound generated aerodynamically I. General theory. *Proc. R. Soc. London A* **211**, 564–587.

Lighthill, M. J. 1954 On sound generated aerodynamically II. Turbulence as a source of sound. *Proc. R. Soc. London A* **222**, 1–32.

Lilley, G. M. 1974 On the noise from jets. *AGARD CP-131*.

Morley, A. W. 1939 Estimation of aeroplane noise level: some empirical laws with an account of the present experiments on which they are based. *Aircr. Eng.* **11** (123), 187–189.

NORUM, T. D. & SEINER, J. M. 1982 Measurements of mean static pressure and far-field acoustics of shock-containing supersonic jets. *NASA TM-84521*.

RAY, P. K., CHEUNG, L. C. & LELE, S. K. 2004 On sound generated by instability wave-shock cell interaction in supersonic jets. *AIAA-2004-2950*.

SEINER, J. M. & NORUM, T. D. 1979 Experiments of shock associated noise on supersonic jets. *AIAA-79-1526*.

SEINER, J. M. & NORUM, T. D. 1980 Aerodynamic aspects of shock containing jet plumes. *AIAA-80-0965*.

SEINER, J. M. & YU, J. E. 1981 Acoustic near field and local flow properties associated with broadband shock noise. *AIAA-81-1975*.

STANESCU, D. & HABASHI, W. G. 1998 $2N$-Storage low dissipation and dispersion Runge-Kutta schemes for computational aeroacoustics. *J. Comp. Phys.* **143**, 674–681.

TAM, C. K. W. 1987 Stochastic model theory of broadband shock associated noise from supersonic jets. *J. Sound Vib.* **116**, 265–302.

TAM, C. K. W. 1990 Broadband shock-associated noise of moderately imperfectly expanded supersonic jets. *J. Sound Vib.* **140**, 55–71.

TAM, C. K. W. 1995 Jet noise generated by large-scale coherent motion. In *Aeroacoustics of Flight Vehicles: Theory and Practice. Volume I: Noise Sources*. NASA Langley Research Center, Hampton, Virginia.

TAM, C. K. W., JACKSON, J. A. & SEINER, J. M. 1985 A Multiple-scales model of the shock-cell structure of imperfectly expanded supersonic jets. *J. Fluid Mech.* **153**, 123–149.

TAM, C. K. W. & TANNA, H. K. 1982 Shock associated noise of supersonic jets from convergent-divergent nozzles. *J. Sound Vib.* **81**, 337–358.

TANNA, H. K. 1977*a* An experimental study of jet noise part I: turbulent mixing noise. *J. Sound Vib.* **50**, 405–428.

TANNA, H. K. 1977*b* An experimental study of jet noise part II: shock associated noise. *J. Sound Vib.* **50**, 429-444.

TITZE, I. R. 2000 *Principles of Voice Production*, 2nd edn. Iowa City, IA: National Center for Voice and Speech.

VISWANATHAN, K. 2004 Aeroacoustics of hot jets. *J. Fluid Mech.* **516**, 39-82.

VISWANATHAN, K. & CLARK, L. T. 2004 Effect of nozzle internal contour on jet aeroacoustics. *Inter. J. Aeroacoustics* **3**, 103–135.

WESTLEY, R. & LILLEY, G. M. 1952 An investigation of the noise field from a small jet and methods for its reduction. *Tech. Rep. 53*, College of Aeronautics, Cranfield, England, UK.

WITZE, P. O. 1974 Centerline velocity decay of compressible free jets. *AIAA J.* **12**, 417-418.